J South Med Univ, 2016, 36(5): 595-603 doi 10.3969/j.issn.1673-4254.2016.05.01

Original Article

Proteomic analysis of retinal proteins in rabbits following intravitreal PBS injection: analysis with tandem mass tag labeling coupled with LC-MS/MS

WANG Jiaming, LEI Bo

Department of Ophthalmology, the First Affiliated Hospital of Chongqing Medical University, Chongqing Key Laboratory of Ophthalmology, Chongqing Eye Institute, Chongqing 400016, China

Abstract: **Objective** Intravitreal (IVT) injection has become one of the most commonly performed ophthalmologic procedures. We investigated the changes in retinal function and proteomics in rabbits receiving IVT injection of PBS to evaluate the safety of IVT injection. **Methods** Twenty Chinchilla rabbits were subjected to IVT injection of 50 μL PBS in the right eyes. On days 0, 4, 7 and day 14, the retinas of the rabbits were isolated after routine ophthalmic and electroretinogram examinations. The protein expressions in the retinas were quantified using tandem mass tag (TMT)-labeling coupled with LC-MS/MS, and bioinformatic analysis of the differentially expressed proteins (DEPs) was performed based on KEGG database to identify significantly enriched pathways. Functional network of the significant DEPs was analyzed using STRING. **Results** No noticeable fundus or functional changes occurred in the rabbit eyes following IVT injection of PBS. A total of 6042 retinal proteins were identified in the retina following the injection, among which 49 proteins (0.81%) exhibited over 5.0-fold up-regulation or over 80% down-regulation relative to the control. Most of the distinctly up-regulated or down-regulated proteins were associated with the cytoskeleton. Significantly enriched pathways involved focal adhesion, tight junction, riboflavin metabolism, extracellular matrix-receptor interaction and regulation of actin cytoskeleton. Functional network analysis showed that ACTC1 and ISG15 played central roles in the protein interaction networks. **Conclusion** IVT PBS injection in rabbits causes alterations in proteins associated with cell adhesion, morphology, migration, differentiation, signal transduction and riboflavin metabolism, but the alterations of the retinal proteins appear not sufficient to cause observable pathology of the retina.

Key words: intravitreal injection; retina; proteomics; tandem mass tags

INTRODUCTION

Intravitreal (IVT) injection of anti-vascular endothelial growth factor (anti-VEGF) agents has become the first-line treatment for neovascular retinal diseases, and IVT injection of steroids is also commonly used for treating several eye diseases. It is estimated that nearly 6 million injections will be carried out in the United States in 2016 [1]. With the establishment and expansion of the procedural standards, IVT injection has been shown to be safe in most cases, but in occasional cases, the patients are still exposed to a cumulative risk of intraocular noninfectious events and other complications associated with IVT injection [2]. Whether the complications are caused by the drugs injected or by the procedure itself remains unknown. Investigation of the effects of a single IVT injection without drugs on retinal proteomics may both provide valuable insights in understanding the injection procedure-associated adverse effects and yield important data for optimizing the clinical therapeutic regimen to lower the incidence of the adverse events. Indeed, a recent report has demonstrated that the procedure of a single IVT injection of PBS alone is sufficient to cause substantial reactive changes in Müller cells and microglia involving the entire retina of mice[3].

To explore the subclinical effects of IVT injection on the retina, we analyzed the changes of retinal proteins using tandem mass tag (TMT)-labeling coupled with quantitative mass spectrometry. Such a proteomic study may produce data that enable the identification of the proteins, functions and pathways potentially responsible for the adverse effects of the IVT procedure, other than the drugs injected.

MATERIALS AND METHODS

Animal grouping and treatment

All the experiments were conducted in accordance with the Association of Research in Vision and Ophthalmology (ARVO) Statement for the Use of Animals in Ophthalmic and Vision Research and were approved by the Ethics Committee of the First Affiliated Hospital of Chongqing Medical University (Chongqing, China). Twenty pigmented Chinchila rabbits weighing 2

Received: 2016-02-19 **Accepted:** 2016-04-10

Supported by National Natural Science Foundation of China (81470621).

Corresponding author: LEI Bo, MD, PhD, Tel: 023-89011851, e-mail: bolei99@126.com.

to 3 kg were kept in an air-conditioned room (20-25 ℃) with a 12-hour light-dark cycle and fed with standard laboratory food and water. The rabbits were randomized into 4 groups (n=5), including a control group (group A) without receiving any injection and 3 IVT injection groups, which received IVT injection of 50 μL PBS and were sacrificed at 4, 7, and 14 days later (groups B, C, and D, respectively). In the latter 3 groups, only the right eye of each rabbit was subjected to IVT injection.

Intravitreal injection

IVT injection was performed under sterile conditions. The rabbits were anesthetized with an injection of 3% pentobarbital sodium solution (30 mg/kg) via the ear vein. After topical corneal anesthesia with oxybuprocaine hydrochloride eye drops (Santen Pharmaceutical Co., Ltd, Osaka, Japan), a 27-gauge needle attached to a 1-mL syringe was introduced into the vitreous cavity 3.5 mm posterior to the limbus. The needle tip was directed towards the center of the vitreous under direct vision. PBS (50 μL) was slowly administered into the vitreous. To prevent reflux, the needle was held in place for 30 s before withdrawal. At the end of the procedure, lincomycin eye drops were applied.

Fundus photography and electroretinography

Fundus photography of the rabbit eye was performed using a digital slit lamp with a 70-diopter lens (Volk Optical Inc, Ohio, USA) under anesthesia. Electroretinogram (ERG; RetiMINER System, AiErXi Medical Equipment Co., Ltd., Chongqing, China) was recorded on days 4, 7, and 14 after IVT injection. Briefly, the rabbits were anesthetized with pentobarbital sodium, and after the pupils had been dilated, Burian-Allen electrodes (Hansen Laboratory, Iowa City, Iowa) were applied. The ground electrode was placed subcutaneously on the back. Dark- and light-adapted ERGs were recorded following the procedure described previously[4].

Retinal protein extraction

Retinas were isolated from the eyeballs, frozen in liquid nitrogen, and lysed using a protein extraction buffer (8 mol/L urea, 0.1% SDS) containing a protease inhibitor cocktail (Roche, Indianapolis, IN, USA) on ice for 30 min. After centrifugation of the lysate at 16 000×g for 15 min at 4 ℃, the supernatant was collected and protein concentration was determined using a BCA protein assay kit (Pierce, Rockford, IL, USA).

TMT-labeling and fractionation of labeled peptides

TMT-labeling was performed according to the manufacturer's instructions (Pierce). Triethylammonium bicarbonate (TEAB) buffer (100 mmol/L) was added to the protein solution (100 μg total protein) to a final volume of 100 μL. Five microliters of tris-(2-carboxyethyl)phosphine (TCEP; 200 mmol/L) was added to the solution, which was incubated at 55 ℃ for 1 h. Immediately before use, fresh 375 mmol/L iodoacetamide solution was prepared (by dissolving 9 mg iodoacetamide in 132 μL of 100 mmol/L TEAB) and 5 μL of the iodoacetamide solution was added to the sample and incubated for 30 min in darkness at room temperature. The proteins were precipitated by pre-chilled (−20 ℃) acetone. After resuspension, the proteins were digested overnight at 37 ℃ with 2.5 μg of trypsin. One tube of TMT10 label reagent was added to each 100 μg sample, and the reaction was carried out at room temperature for 1 h. The labeling reaction was quenched by adding 8 μL of 5% hydroxylamine. After labeling, the samples from 3 retinas in each group were mixed for measurement.

For fractionation of the labeled peptides, the samples were first lyophilized and reconstituted in solvent A (2% ACN, pH10). The samples were then loaded onto Xbridge PST C18 column (130 Å, 5 μm, 250 mm×4.6 mm column; Waters, Milford, MA, USA) and resolved by basic reversed-phase liquid chromatography (RPLC) using a gradient of 5% to 95% solvent B (90% ACN, pH10) in 40 min. A total of 40 fractions were collected, which were concatenated to 20 fractions, vacuum dried and stored at −80℃ until analysis.

Liquid chromatography-tandem mass spectrometry

Liquid chromatography-tandem mass spectrometry (LC-MS/MS) analysis was carried out by Capitalbio Technology with a Q Exactive Mass Spectrometer (Thermo Scientific, San Jose, CA). The peptide mixture was separated by reversed phase chromatography on a DIONEX nano-UPLC system using an Acclaim C18 PepMap100 nano-Trap column (75 μm × 2 cm) connected to an Acclaim PepMap RSLC C18 analytical column (75 μm×25 cm, particle size of 2 μm; Thermo Scientific). Before loading, the sample was dissolved in a buffer containing 4% acetonitrile and 0.1% formic acid. A linear gradient of mobile phase B (0.1% formic acid in 99.9% acetonitrile) from 2% to 35% in 45 min was used followed by a steep increase to 80% mobile phase B in 1 min at a flow rate of 300 nL/min. The nano-LC was coupled online with the Q Exactive mass spectrometer using a stainless steel emitter coupled to a nanospray ion source.

Mass spectrometry analysis was performed in a data-dependent manner with full scans (300-1800 m/z) acquired using an Orbitrap mass analyzer at a mass resolution of 70 000 at 400 m/z in Q Exactive. Twenty most intense precursor ions from a survey scan were selected for MS/MS from each duty cycle and detected at a mass resolution of 35 000 at m/z of 400 in Orbitrap analyzer. All the tandem mass spectra were produced by higher-energy collision dissociation (HCD) method. Dynamic exclusion was set for 20 s.

Analysis of enriched pathway

Enriched pathways were analyzed with the command-line program KOBAS 2.0. We used the whole genome as the default background distribution to

identify the significantly enriched pathways in a set of sequences. For each pathway that occurred in the set of genes, we counted the total number of genes involved in the set. We calculated the p value using a hypergeometric distribution. If a whole genome has N total genes, among which M are involved in the pathway under investigation, and the set of genes has n total genes, among which m are involved in the same pathway, the p value for the pathway was calculated as below:

$$p = 1 - \sum_{i=0}^{m-1} \frac{\binom{m}{i}\binom{N-M}{n-i}}{\binom{N}{n}}$$

Because a large number of KEGG pathways are considered, multiple hypotheses tests are performed. To reduce the type-1 errors (i.e. false positive discoveries), we performed an FDR correction with a default cutoff of 0.05.

Analysis of protein-protein interactions

Protein-protein interactions were analyzed using the web-based bioinformatic search software STRING (version 9.1). STRING contains a database of interactions for known or predicted proteins including physical and functional associations from genomic contexts, high-throughput experiments, coexpression and previous knowledge. The significantly changed proteins were entered into STRING for analyzing the protein interactions. The background set was the full *Oryctolagus* proteome.

Data analysis

Proteome Discoverer software (Ver. 1.4, Thermo Scientific) was used to perform database searching against the Oryctolagus Cuniculus database (46551 proteins) using the Sequest algorithms. The following settings were used: precursor mass tolerance of 15 mg/kg, and fragment mass tolerance of 0.02 Da. Trypsin was specified as the digesting enzyme and 2 missed cleavages were allowed. Cysteine carbamidomethylation and TMT modifications (N-terminus and lysine residues) were defined as fixed modifications and methionine oxidation was defined as variable modifications. The results were filtered by including only the highly confident peptides with a global FDR<1% based on a target-decoy approach. In the TMT quantitation workflow the most confident centroid method was used with an integration window of 20 mg/kg. For protein quantification, only unique peptides were used.

Statistical analysis

Statistical analysis was performed using the GraphPad Prism (GraphPad Prism 5, Inc., San Diego, CA, USA). The results were analyzed by one-way ANOVA followed by Bonferroni correction for multiple comparisons. A P value less than 0.05 was considered to indicate a statistically significant difference.

RESULTS

Ophthalmic and ERG examinations

Before and after IVT injection, fundus and ERG examinations were performed. Fundus photography detected no distinct changes in the eyes after injection as compared to the untreated control eyes (Fig.1). Fig.2 shows the representative ERG responses and amplitude-intensity profiles of the untreated control and the PBS-injected eyes. The ERG waveforms and the amplitudes of the averaged a- and b-wave recorded under various stimuli in the PBS-injected groups were similar with those obtained in the control groups (P> 0.05, n=5).

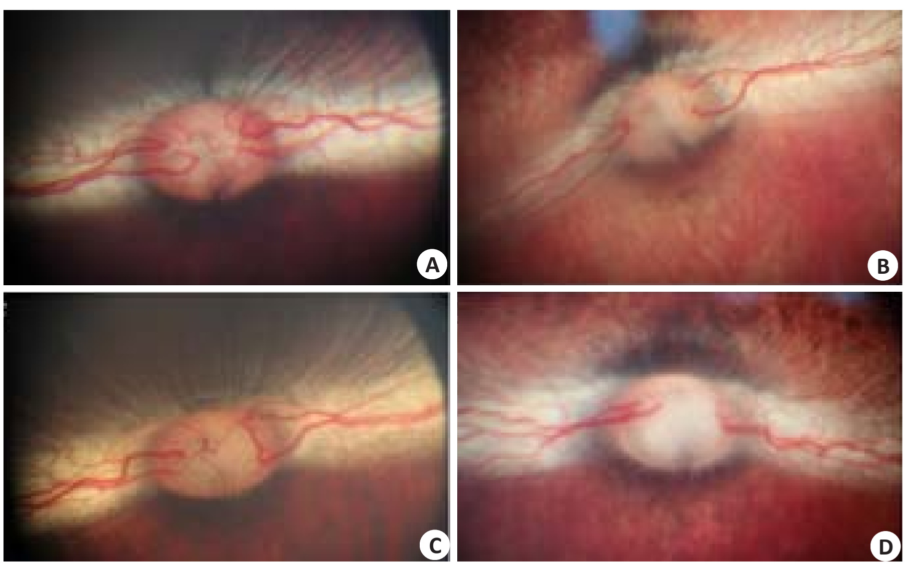

Fig.1 Fundus photography of rabbit eyes after IVT injection of PBS. ***A***: A representative untreated control eye; ***B***, ***C***, **D**: PBS injected eyes on days 4, 7, 14 after the injection, respectively. No obvious abnormality was found in the injected eyes as compared with the control eye.

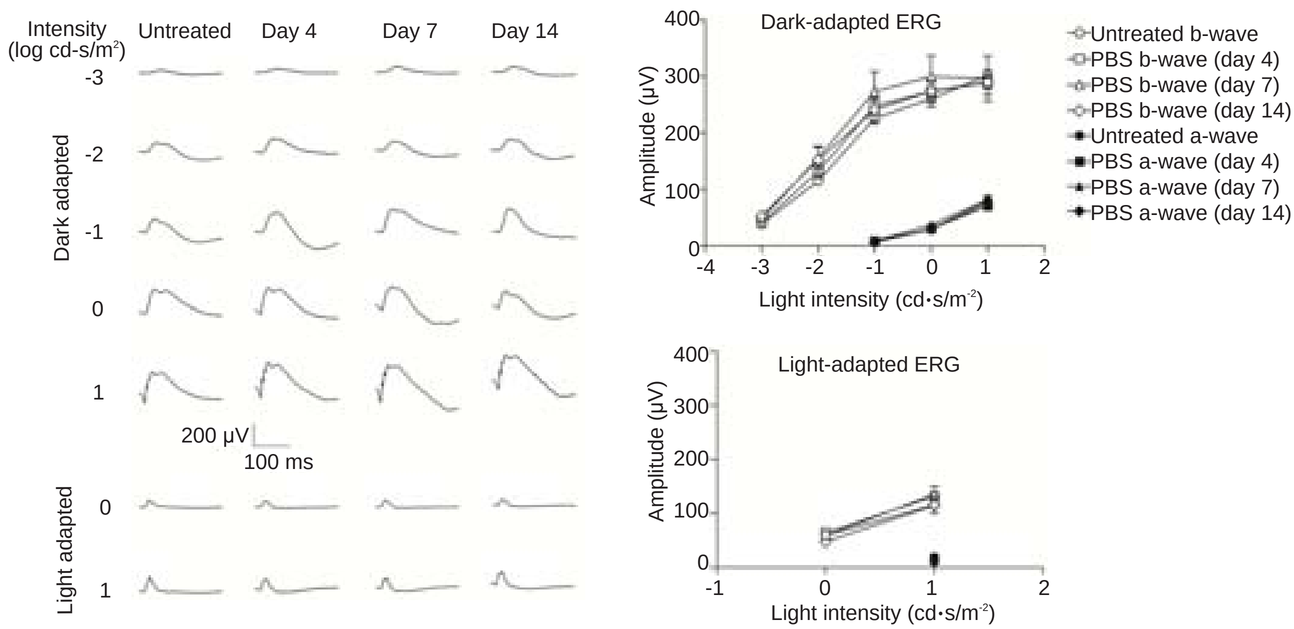

Fig.2 ERG waveforms and amplitude-intensity profiles of the rabbit eyes after IVT injection of PBS. No significant difference was found in the amplitudes of a- and b-waves among the groups (P>0.05, n=5).

Protein profile

The proteins identified from rabbit retinas had a wide range of relative molecular masses (from 4000 to 1 000 000 Da). Most of proteins had a *pI* between 4 and 12. To improve the analytical precision, all the quantitative data related to a certain peptide that was identified in multiple fractions were used for deriving the protein quantification tables. We obtained a total of 6042 proteins from the rabbit retinas. Among them, 155 differentially expressed proteins (DEPs) from the injected eyes were up-regulated by more than 2 folds or down-regulated by over 50% relative to the control. These DEPs included 19 proteins up-regulated by over 5 folds (Tab.1), 14 down-regulated by over 80% (Tab.2), and 16 with inconsistent changes at different time points (Tab.3).

Proteomics quantification analysis

Among the 6042 proteins, actin, alpha cardiac muscle 1 was the most prominently up-regulated protein (by 36.91 folds) in the retina at 7 days after IVT injection of PBS, followed by lactotransferrin and sarcoplasmic/endoplasmic reticulum calcium ATPase 1, which were up-regulated by over 10 folds at days 4 and 7 (Tab.1). The most distinctly down-regulated protein was carbonyl reductase [NADPH] 3, which was expressed at only 9% of the control level at day 14 after the injection (Tab.2).

Functional enriched pathway of DEP

To better understand the functions of the DEPs, we performed pathway analysis using KOBAS 2.0 software based on KEGG database. Twenty significantly enriched pathway terms are shown in Fig.3. KEGG analysis indicated that the DEPs were involved in pathways of glycan degradation, focal adhesion, cytosolic DNA-sensing pathway, arginine and proline metabolism, tight junction, riboflavin metabolism, RIG-I-like receptor signaling pathway, ECM-receptor interaction, steroid biosynthesis, steroid biosynthesis, glycosaminoglycan degradation, glycerophospholipid metabolism, protein digestion and absorption, regulation of actin cytoskeleton, PI3K-Akt signaling pathway, lysosome, leukocyte transendothelial migration, and SNARE interactions in vesicular transport.

Functional network of DEPs

Through the protein-protein interaction network, we identified the proteins involved in the biological processes including signal transduction, regulation of gene expression, energy and material metabolism, and cell cycle regulation. Analysis against BioGrid database showed the interactions between the DEPs (Fig.4). Using functional network diagram analysis, we found that 46 proteins were involved in functional and physical connections. In this network, DEPs and one-step interacting proteins were represented as nodes, and the biological relationship between two nodes was represented as an edge. The size of the node is proportional to the degree of association: the more edges are connected to the node, the greater the degree of association, and the bigger the size of the node. The color of the node, from green to red, corresponds to the value of the clustering coefficient gradient (from low to high) that indicates the connectivity between the nodes. The diagram in Fig.4 highlights 46 nodes and 74 edges, forming 53 DEP-DEP pairs. ISG15 and ACTC1 are two genes encoding ubiquitin-like protein ISG15 and actin, alpha cardiac muscle 1, respectively, to which 13 and 9 one-step interacting proteins are connected,

Tab.1 Significantly up-regulated proteins in the retina of rabbits with IVT injection of PBS

Accession number	Gene symbol	Protein name	Fold change (IVT injection *vs* control)		
			Day 4	Day 7	Day 14
291403287	ACTC1	Actin, alpha cardiac muscle 1	1.05	36.91	1.12
655857145	BMPR1B	Bone morphogenetic protein receptor type-1B isoform X2	2.97	7.02	6.38
655841362	KLHDC3	Kelch domain-containing protein 3	3.05	7.31	3.42
655834100	LTF	Lactotransferrin	10.83	1.05	1.61
147903853	ATP2A1, ATP2A3 SERCA1a	*Sarcoplasmic/endoplasmic reticulum calcium atpase 1	1.12	10.93	1.03
655855155	NFKBIZ, Mail	NF-kappa-B inhibitor zeta isoform X2	2.82	2.96	6.33
655834754	RBM15B	Putative RNA-binding protein 15B	3.93	4.47	3.57
655833765	MKRN2	Probable E3 ubiquitin-protein ligase makorin-2 isoform X5	6.67	3.06	1.84
655600655	VPS13A	Vacuolar protein sorting-associated protein 13A	2.71	6.65	2.05
655866440	PBLD	Phenazine biosynthesis-like domain-containing protein isoform X2	2.89	1.53	4.81
130501699	MYLPF	*Myosin regulatory light chain 2, skeletal muscle isoform type 2	1.15	6.27	1.03
655860575	IKBKE	Inhibitor of nuclear factor kappa-B kinase subunit epsilon	1.08	5.35	1.04
655862947	GATM	LOW QUALITY PROTEIN: glycine amidinotransferase, mitochondrial	2.37	1.05	2.57
655893954	HEXDC	Hexosaminidase D	2.06	2.27	1.65
655882768	CRYBB1	Beta-crystallin B1	2.73	1.23	1.97
655846332	GBA	Glucosylceramidase isoform X2	2.17	1.35	2.08
315360675	EPT1, SELI	Ethanolaminephosphotransferase 1	1.89	1.49	2.04
129270090	CRYAA	Alpha-crystallin A chain	3.04	1.10	1.25
291410889	PGER6	Prostaglandin-E(2) 9-reductase	1.08	1.22	2.80

*Not predicted protein.

Tab.2 Significantly down-regulated proteins in the retina of rabbits with IVT injection of PBS

Accession number	Gene symbol	Protein name	Fold change (IVT injection *vs* control)		
			Day 4	Day 7	Day 14
291410032	CBR3	Carbonyl reductase [NADPH] 3	0.59	0.51	0.09
291389187		Keratin, type II cuticular Hb6	0.23	0.32	0.13
655872869	KRT34	LOW QUALITY PROTEIN: keratin, type I cuticular Ha4	0.23	0.34	0.18
291393010	LACC1	Laccase domain-containing protein 1	0.50	0.39	0.12
655879141	UBL3	Ubiquitin-like protein 3	0.70	0.26	0.17
291402469	HSD11B1	Corticosteroid 11-beta-dehydrogenase isozyme 1	0.43	0.42	0.30
291402773	ITGA11	Integrin alpha-11	0.43	0.50	0.41
655842073	MB21D1	Cyclic GMP-AMP synthase	0.14	0.76	0.47
291409274		1,25-dihydroxyvitamin D(3) 24-hydroxylase, mitochondrial	0.64	0.50	0.41
655601432		FXYD domain-containing ion transport regulator 6 isoform X3	0.77	0.12	0.83
655901361	ISG15	Ubiquitin-like protein ISG15	0.63	0.63	0.50
655871442		LOW QUALITY PROTEIN: tubulin gamma-2 chain-like	0.81	0.55	0.44
655600642	RFK	Riboflavin kinase	0.66	0.43	0.73
291406137	NAGLU	Alpha-N-acetylglucosaminidase	0.49	0.57	0.86

Tab.3 Inconsistent changes in the expression levels of the retinal proteins at days 4, 7, and 17 after IVT injection

Accession number	Gene symbol	Protein name	Fold-change (IVT injection *vs* control)		
			Day 4	Day 7	Day 14
157787195	TPM2	*Tropomyosin 2 (beta)	0.77	28.23	1.01
156119398	MYL1	*Myosin light chain 1/3, skeletal muscle isoform	0.78	23.13	0.79
655902632	TNNT1	Troponin T, slow skeletal muscle	0.25	19.95	0.78
130493079	TNNI2, TnI	*Troponin I, fast skeletal muscle	0.24	17.83	0.84
655868632		Myosin-2	0.78	17.93	0.84
126723052	CASQ1	*Calsequestrin-1 precursor	0.62	10.27	0.97
655886422	MYLPF	Myosin regulatory light chain 2, skeletal muscle isoform type 2	0.59	9.42	0.54
655758942	MYBPC1	Myosin-binding protein C, slow-type, partial	0.74	8.12	0.62
291402113	ACTN2	Alpha-actinin-2	0.95	7.65	1.05
157787199	TPM1, TPMA	*Tropomyosin alpha-1 chain	1.25	5.89	0.94
655889682	CASP9	LOW QUALITY PROTEIN: caspase-9	0.57	1.90	3.82
126723370	CKM	*Creatine kinase M-type	0.99	2.65	0.78
655884547	FLT1	Vascular endothelial growth factor receptor 1	0.32	1.16	1.62
291410404	KCNJ13, KIR7.1	Inward rectifier potassium channel 13 isoform X1	0.99	2.00	2.10
655847855	COL11A1	Collagen alpha-1(XI) chain isoform X1	0.58	1.20	0.46
291394806	BET1	BET1 homolog	0.95	1.19	0.49

*Not predicted protein.

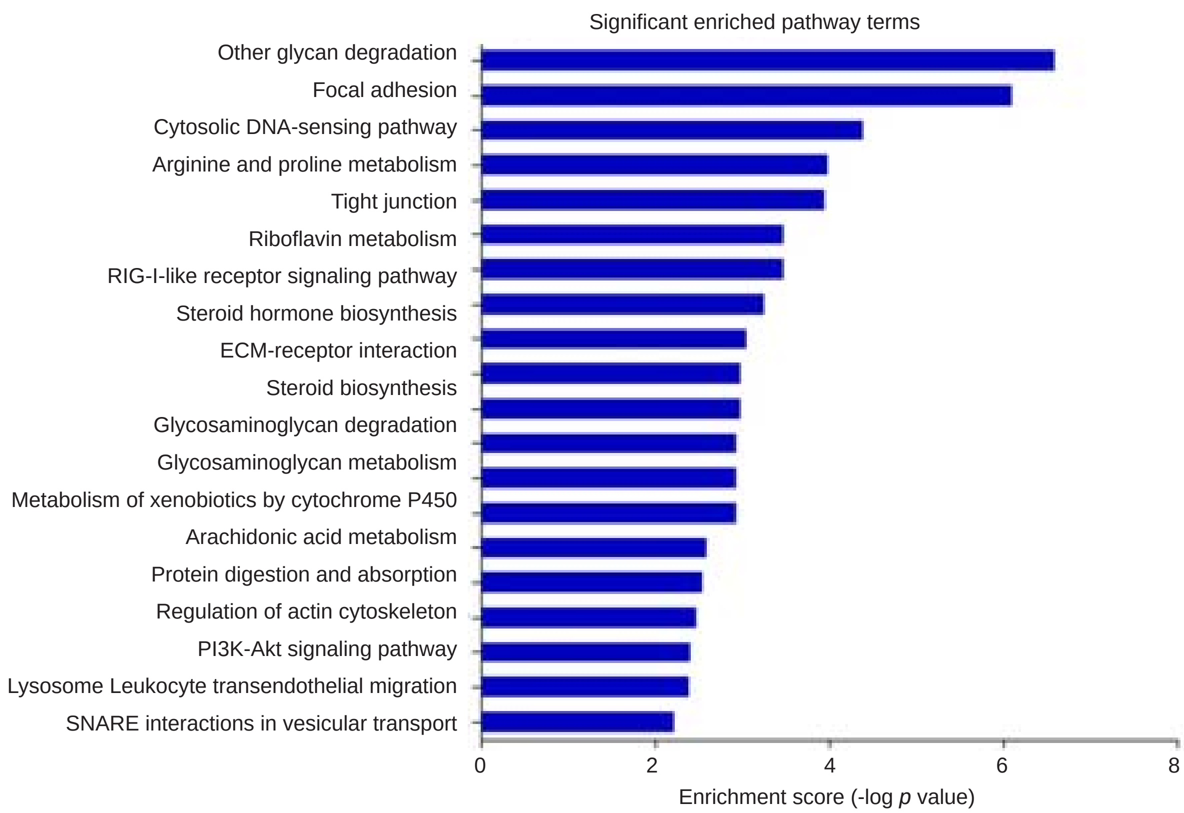

Fig.3 Functional enriched pathways of DEPs in the retina of rabbit eyes with IVT injection of PBS. Bioinformatic analysis of retinal proteomics was performed based on KEGG database and 20 enriched pathways were identified. The -log of *P* value was calculated by Fisher's exact test.

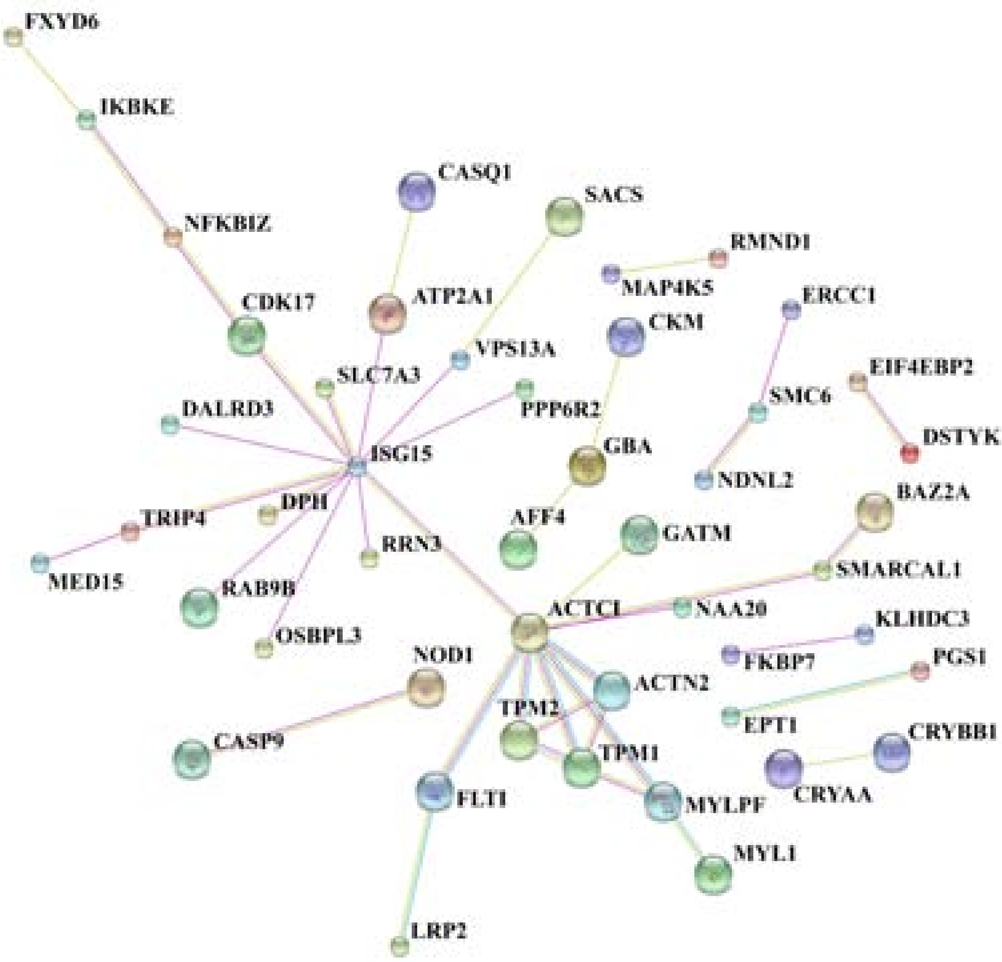

Fig.4 Biological interaction network of DEPs in the retina of rabbits with IVT PBS injection. Proteins are represented as nodes and the biological relationship between two nodes is shown as an edge. There are 46 nodes and 74 edges, including 53 DEP-DEP pairs.

respectively. Among the one-step proteins connected to actin, alpha cardiac muscle 1, tropomyosin alpha-1 chain, tropomyosin 2 (beta) and alpha-actinin-2 interact with each other directly and form a triangle interaction network.

DISCUSSION

In this study, TMT-labeled proteomic technology was used to analyze the alterations of the retinal proteins after IVT injection of PBS in rabbits. Due to its fast separation, high sensitivity and high resolution, this technique has become a powerful method to identify the DEPs with a large coverage of the proteome. To our knowledge, the current study represents the first attempt to apply this method in the exploration of DEPs in the retina following IVT injection. Although our proteomic analysis was based on a database of rabbit proteins, it may help in better understanding retinal protein alternations after IVT injection and in discovering the proteins that are specifically associated with the IVT procedure. The differential expression of retinal proteins following IVT injection are probably related with the retinal wound induced by the needle puncture, PBS injected, or a transient elevation of the intraocular pressure, all of which are inevitable consequences after an IVT injection.

Our analysis identified a total of 6042 proteins in the retina, and among them 49 proteins (0.81%) were up-regulated by over 5.0 folds or down-regulated by over 80% (with a probability greater than 95.0%) at 4, 7 or 14 days after IVT injection of PBS. The most striking DEPs caused by IVT injection were associated with cytoskeleton alterations. Cytoskeleton plays a vital role in sustaining the growth, maturation, differentiation, and integrity of cells in the eye[5]. Among the cytoskeleton-related proteins, actin, alpha cardiac muscle 1 was the most remarkably changed protein, and protein interaction network analysis indicated a central role for ACTC1 gene, which encodes this protein.

The signaling pathway of focal adhesion was altered in the injected eyes. Proteins involved in focal adhesion included collagen alpha-1(XI) chain isoform X1, vascular endothelial growth factor receptor 1, integrin alpha-11, myosin regulatory light chain 2, skeletal muscle isoform type 2 and alpha-actinin-2, among which collagen alpha-1(XI) chain isoform X1 and integrin alpha-11 were also involved in extracellular matrix (ECM)-receptor interaction pathway. Focal adhesions are large macromolecular assemblies that

function as signal carriers by delivering messages to the cells and subsequently affect the cell behaviors [6]. Connection between focal adhesions and proteins of the ECM generally involves integrins. Composed of α and β subunits, integrins are transmembrane heterodimers that transmit signals from the ECM to the cells [7, 8] and mediate stable adhesion of cells to their substrate[9]. More importantly, integrins trigger signaling cascades from the ECM into the cell to control crucial cellular functions including cell differentiation, proliferation, survival and migration[10, 11]. In the eye, the ECM provides a framework for retinal cells, and adhesion junctions connect the cells via the core components including actin[12]. Clustering and activation of integrins and actin complexes initiate this framework for cell signaling [13]. In our study, down-regulation of integrin alpha-11 was detected at all the 3 time points in the injected eyes, indicating functional disorder of cell adhesions and potential defects in the morphology, migration and differentiation of retinal cells. In addition, IVT injection also up-regulated the tight junction pathway, which was modulated by a variety of cellular and metabolic regulators [14]. We noted an evident increase of alpha-actinin-2, which is involved in both focal adhesion signaling and tight junction pathways and plays a key role in controlling integrin activation and its binding to cytoskeleton within the cell[15].

We also identified changes in riboflavin (RF) metabolism in the retina following IVT injection. IVT injection down-regulated the expression of riboflavin kinase (RFK) in the retina. RF (known also as water-soluble vitamin B2) is vital in maintaining the structural and functional integrity of the ocular surface [16], photoreceptors and lens[17, 18]. RF is transformed into its active coenzyme derivatives by phosphorylation of an ATP:riboflavin kinase, which catalyses RF into flavin mononucleotide (FMN), and the latter was further catalyzed into flavin adenine dinucleotide (FAD) by FAD synthetase (FADS) [19]. FMN and FAD are two essential cofactors for numerous enzymes contributing to the transfer of electrons in oxido-reduction processes critical to the major metabolic energy transformation routes [20, 21]. FAD also mediates the regeneration of reduced glutathione, which is the major regulator of the intracellular thiol redox status and effectively scavenges free radicals and other reactive oxygen species (ROS)[22]. The down-regulation of RFK, which is a crucial point of RF transformation into FMN and FAD and a key step in the biological oxidation-reduction reactions, implies that this metabolic pathway is affected after IVT injection.

The level of lactotransferrin (LF) increased by nearly 11 folds at day 4 after IVT injection. LF is an important component in the host defense system in ocular tissues[23]. It is associated with therapeutic effects by promoting corneal wound healing, restoring loss of corneal epithelial integrity and reducing chorioretinal damage [24-27], and is related with protection against infection, tumor and inflammation in the eye [28, 29]. Elevation of retinal LF in eyes following IVT injection seems to imply the activation of the local protective mechanism in the retina.

Our data did not show any changes of inflammatory cytokines or chemokines in PBS-injected eyes, but we detected an increase in the expression of caspase-9 in the retina by 1.9 and 3.82 folds at days 7 and 14 after the injection, respectively. Caspase-9 is an initiator caspase activated by apoptosome during programmed cell death[30, 31]. We also noted a remarkable increase of NF-kappa-B inhibitor zeta isoform X2, but its exact role in the process of inflammation and apoptosis is yet unclear. Previous studies have identified it as an atypical nuclear member of the IκB family with dual functions in positive and negative regulation of NF-κB-mediated transcription[32-34].

In conclusion, we found significant alternations in the expression profiles of retinal proteins associated with cell adhesion, morphology, migration, differentiation, signal transduction and riboflavin metabolism in rabbit eyes after IVT PBS injection. Although these changes did not appear to be sufficient to cause tangible bodily signs, they testify the fact that IVT injection is at least capable of causing retinal changes at the protein level.

REFERENCES

[1] Avery RL, Bakri SJ, Blumenkranz MS, et al. Intravitreal injection technique and monitoring: updated guidelines of an expert panel[J]. Retina, 2014, 34 (Suppl 12): S1-18.

[2] Kelly SP, Barua A. A review of safety incidents in England and Wales for vascular endothelial growth factor inhibitor medications [J]. Eye (Lond), 2011, 25 (6): 710-6.

[3] Seitz R, Tamm ER. Muller cells and microglia of the mouse eye react throughout the entire retina in response to the procedure of an intravitreal injection[J]. Adv Exp Med Biol, 2014, 801: 347-53.

[4] Zhang K, Yao G, Gao Y, et al. Frequency spectrum and amplitude analysis of dark- and light-adapted oscillatory potentials in albino mouse, rat and rabbit[J]. Doc Ophthalmol, 2007, 115: 85-93.

[5] Bozanic D, Bocina I, Saraga-Babic M. Involvement of cytoskeletal proteins and growth factor receptors during development of the human eye[J]. Anat Embryol (Berl), 2006, 211: 367-77.

[6] Riveline D, Zamir E, Balaban NQ, et al. Focal contacts as mechanosensors: externally applied local mechanical force induces growth of focal contacts by an mDia1-dependent and ROCK-independent mechanism[J]. J Cell Biol, 2001, 153: 1175-86.

[7] Mettouchi A, Meneguzzi G. Distinct roles of beta1 integrins during angiogenesis[J]. Eur J Cell Biol, 2006, 85: 243-47.

[8] Huveneers S, Danen EH. Adhesion signaling- crosstalk between integrins, Src and Rho[J]. J Cell Sci, 2009, 122: 1059-69.

[9] Bokel C, Brown NH. Integrins in development: moving on, responding to, and sticking to the extracellular matrix [J]. Dev Cell, 2002, 3: 311-21.

[10] Giancotti FG, Ruoslahti E. Integrin signaling[J]. Science, 1999, 285: 1028-32.

[11] Takada Y, Ye X, Simon S. The integrins[J]. Genome Biol, 2007, 8: 215.

[12] Mirkovic I, Mlodzik M. Cooperative activities of drosophila DE-cadherin and DN-cadherin regulate the cell motility process of ommatidial rotation[J]. Development, 2006, 133: 3283-93.

[13] Kim SH, Turnbull J, Guimond S. Extracellular matrix and cell signalling: the dynamic cooperation of integrin, proteoglycan and growth factor receptor[J]. J Endocrinol, 2011, 209: 139-51.

[14] Yang X, Liu B, Bai Y, et al. Elevated pressure downregulates ZO-1 expression and disrupts cytoskeleton and focal adhesion in human trabecular meshwork cells[J]. Mol Vis, 2011, 17: 2978-85.

[15] Stanley P, Smith A, McDowall A, et al. Intermediate-affinity LFA-1 binds alpha-actinin-1 to control migration at the leading edge of the T cell[J]. EMBO J, 2008, 27: 62-75.

[16] Takami Y, Gong H, Amemiya T. Riboflavin deficiency induces ocular surface damage[J]. Ophthalmic Res, 2004, 36: 156-65.

[17] Miyamoto Y, Sancar A. Vitamin B2-based blue-light photoreceptors in the retinohypothalamic tract as the photoactive pigments for setting the circadian clock in mammals[J]. Proc Natl Acad Sci USA, 1998, 95: 6097-102.

[18] Cumming RG, Mitchell P, Smith W. Diet and cataract: the Blue

Mountains Eye Study[J]. Ophthalmology, 2000, 107: 450-56.
[19] Serrano A, Sebastian M, Arilla-Luna S, et al. Quaternary organization in a bifunctional prokaryotic FAD synthetase: Involvement of an arginine at its adenylyltransferase module on the riboflavin kinase activity[J]. Biochim Biophys Acta, 2015, 1854: 897-906.
[20] Joosten V, van Berkel WJ. Flavoenzymes[J]. Curr Opin Chem Biol, 2007, 11: 195-202.
[21] Serrano A, Frago S, Velazquez-Campoy A, Medina M. Role of key residues at the flavin mononucleotide (FMN): adenylyltransferase catalytic site of the bifunctional riboflavin kinase/flavin adenine dinucleotide (FAD) synthetase from corynebacterium ammoniagenes[J]. Int J Mol Sci, 2012, 13: 14492-517.
[22] Hirano G, Izumi H, Yasuniwa Y, et al. Involvement of riboflavin kinase expression in cellular sensitivity against cisplatin[J]. Int J Oncol, 2011, 38: 893-902.
[23] Rageh AA, Ferrington DA, Roehrich H, et al. Lactoferrin expression in human and murine ocular tissue[J]. Curr Eye Res, 2015: 1-7.
[24] Montezuma SR, Dolezal LD, Rageh AA, et al. Lactoferrin reduces chorioretinal damage in the murine laser model of choroidal neovascularization[J]. Curr Eye Res, 2015, 40: 946-53.
[25] Fujihara T, Nagano T, Nakamura M, et al. Lactoferrin suppresses loss of corneal epithelial integrity in a rabbit short-term dry eye model[J]. J Ocul Pharmacol Ther, 1998, 14: 99-107.
[26] Pattamatta U, Willcox M, Stapleton F, et al. Bovine lactoferrin promotes corneal wound healing and suppresses IL-1 expression in alkali wounded mouse cornea[J]. Curr Eye Res, 2013, 38: 1110-7.
[27] Pattamatta U, Willcox M, Stapleton F, et, al. Bovine lactoferrin stimulates human corneal epithelial alkali wound healing *in vitro*[J]. Invest Ophthalmol Vis Sci, 2009, 50: 1636-43.
[28] Legrand D, Elass E, Carpentier M, et, al. Lactoferrin: a modulator of immune and inflammatory responses[J]. Cell Mol Life Sci, 2005, 62: 2549-59.
[29] Gifford JL, Hunter HN, Vogel HJ. Lactoferricin: a lactoferrin-derived peptide with antimicrobial, antiviral, antitumor and immunological properties[J]. Cell Mol Life Sci, 2005, 62: 2588-98.
[30] Brentnall M, Rodriguez-Menocal L, De Guevara RL, et, al. Caspase-9, caspase-3 and caspase-7 have distinct roles during intrinsic apoptosis[J]. BMC Cell Biol, 2013, 14: 32.
[31] Blanch RJ, Ahmed Z, Thompson AR, et al. Caspase-9 mediates photoreceptor death after blunt ocular trauma[J]. Invest Ophthalmol Vis Sci, 2014, 55: 6350-57.
[32] Motoyama M, Yamazaki S, Eto-Kimura A, et, al. Positive and negative regulation of nuclear factor-kappaB-mediated transcription by IkappaB-zeta, an inducible nuclear protein[J]. J Biol Chem, 2005, 280: 7444-51.
[33] Yamazaki S, Muta T, Takeshige K. A novel IkappaB protein, IkappaB-zeta, induced by proinflammatory stimuli, negatively regulates nuclear factor-kappaB in the nuclei[J]. J Biol Chem, 2001, 276: 27657-62.
[34] Yamamoto M, Yamazaki S, Uematsu S, et al. Regulation of Toll/IL-1-receptor-mediated gene expression by the inducible nuclear protein IkappaBzeta[J]. Nature, 2004, 430: 218-22.

兔玻璃体腔注射PBS后视网膜差异蛋白的表达

汪家名,雷 博
重庆医科大学附属第一医院眼科,眼科学重庆市市级重点实验室,重庆市眼科研究所,重庆 400016

摘要:目的 研究家兔玻璃体腔内注射PBS后的视网膜功能变化及差异蛋白的表达情况以探索玻璃体腔注射的安全性。**方法** 将20只青紫蓝兔随机分为4组,A组不作任何处理,B至D组在兔右眼玻璃体腔内注射50 μL PBS。分别于注射后第0、4、7、14天进行眼底照相和视网膜电图(ERG)检查,之后摘取眼球并分离视网膜。利用串联质谱标签(TMT)联合液相色谱-串联质谱联用(LC-MS/MS)法检测注射组相对于空白对照组的视网膜蛋白变化情况。通过KOBAS及基于KEGG数据库分析明显变化的蛋白富集通路,利用STRING得出明显变化蛋白间相互作用的功能网络图。**结果** 注射组眼底照相结果与空白组相比无明显变化,ERG结果显示视网膜功未受到影响。TMT蛋白质谱共检测出了6042种兔视网膜蛋白,其中49种蛋白(0.81%)在玻璃体腔注射后表达上调超过5倍或下调超过80%。变化比较显著的蛋白主要与细胞骨架有关。显著变化蛋白富集的通路包括黏着斑通路、紧密连接通路、核黄素新陈代谢通路、细胞外基质受体相互作用通路及肌动蛋白细胞骨架调节通路。功能网络图分析显示ACTC1及ISG15在蛋白相互作用关系中起着比较中心的作用。**结论** 玻璃体腔内注射PBS主要引起与细胞黏连、形态、迁移、分化、信号传导及核黄素代谢通路相关的视网膜蛋白变化。

关键词:玻璃体腔注射;视网膜;蛋白质组;串联质谱标签

收稿日期:2016-02-19
基金项目:国家自然科学基金(81470621)
作者简介:汪家名,硕士研究生,E-mail: 38584586@qq.com
通信作者:雷 博,教授,博士,电话:023-89011851,E-mail: bolei99@126.com